

Bifurcation Behavior of Rotation Velocities in Collisional Edge-Plasma with Steep Gradients

U. Daybelge 1), C. Yarim 1), A. Nicolai 2)

1) Istanbul Technical University, Dept. of Aerospace Sciences, Maslak/İstanbul, TURKEY

2) Institut für Plasmaphysik, Forschungszentrum Juelich, Association EURATOM-FZJ,
Trilateral Euregio Cluster, D-52425, Juelich, GERMANY

e-mail contact of main author: daybelge@itu.edu.tr

Abstract. Both poloidal and toroidal plasma rotations of tokamak edge plasma are known to interact with various other mechanisms and thus are related to plasma stability and transport. Solutions for rotation velocities were studied, using a two-time scales system comprising the ambipolarity constraint and the parallel momentum balance equations of the revisited neoclassical theory, with the corrected contribution from also the gyroviscosity tensor. Temperature and density profiles with realistic pedestal forms were considered known and were controlled parametrically. Similarity of this equation system to reaction-diffusion equations were utilized in the numerical simulation and study of critical points on the bifurcation diagram. It was found that the steepness of the density and temperature gradients have important effects on the rotation stability and on its bifurcative behaviour.

1. Introduction

Poloidal and toroidal plasma rotations in tokamak edge are known to interact with various levels of plasma phenomena, involving stability and transport of fields and particles. The coupled rotation velocities in toroidal and poloidal directions were studied recently due to their importance for various other mechanisms, using the two-time scales procedures. Such analyses were based on the ambipolarity constraint and the parallel momentum balance equations of the revisited neoclassical theory [1-4], including the corrections of Mikhailowskii et al., [5] to the gyroviscosity stress tensor. Experimental profiles of temperature and density obtained in machines like Alcator were incorporated in the above analyses as given data after they were approximated analytically by control parameters simulating realistic pedestal forms etc (See Fig.1). Similarity of the equation system used to the system of reaction-diffusion equations were utilized in the numerical simulation and study of critical points on the bifurcation diagram. Discretization of the spatial variable, while taking into account of the radial boundary layer distance from the magnetic separatrix, transforms the partial differential equations of neoclassical plasma into a nonlinear autonomous dynamical system. As in other reaction-diffusion problems [6, 7] (for example, the Brusselator model), the dependent variables are treated, the local rotational velocity components can thus be considered as individual dependent variables of time. The problem is thus reformulated as one, which can be analysed through the behaviour of the system trajectory in the extended multi-dimensional state space of these variables and of the control parameters [8]. Our simulations has shown that the toroidal velocity components at different radial positions do not show a too wide-spread variation, whereas the poloidal velocity is highly position dependent and this dependency becomes more pronounced with the increasing steepness of the temperature profile.

Instead of following the time dependence of toroidal U_ϕ and the poloidal velocities U_θ at individual spatial positions, it is practical to consider a scalar measure of the vector U , comprising all its unknown components. We can, for example, use the norm: $[U] = \|U\|_2 = (U_1^2 + U_2^2 + \dots + U_n^2)^{1/2}$ as referred to in Fig.2. As shown in the figure, decreasing

μ to values less than one, which corresponds to a steepening of the temperature profile in front of the magnetic separatrix, branching behaviour of the fixed points of the system becomes rather complex. There are regions of hysteresis effects, isolas and changes in the number of multi-valuedness. Thus, it is found that the steepness of the density and temperature gradients have important effects on the rotation stability and on its bifurcative behaviour. For a proper understanding of these branches also eigenvalues of the Jacobi matrices at these critical points must be considered. A systematic study shows that at the critical points stability is lost as the temperature profile gets steeper (small μ regions) and merger of different branches suggests an increasing tendency to chaotic behaviour.

2. Basic Equations

Using the notations of former publications [1-4], the governing equations for the described regime are, continuity equation for the ions,

$$\partial_t N_i + J^{-1} \partial_\chi (h_\phi h_\psi \Gamma_{\chi,i}) = S_i^N - J^{-1} \partial_\psi (h_\phi h_\chi \Gamma_{\psi,i}) \quad (1)$$

where $\vec{\Gamma}_i = N_i \vec{U}_i$ and S_i^N are the ion flux and ion particle source, respectively, and momentum balance equation summed over both species:

$$\partial_i (m_i N_i \vec{U}_i) + \nabla \cdot (m_i N_i \vec{U}_i \vec{U}_i) = -\nabla \cdot \vec{\Pi}_i + \vec{J} \times \vec{B} \quad (2)$$

Here $\vec{\Pi}_i$ is the viscosity tensor including $\vec{\Pi}_{0,i}$, $\vec{\Pi}_{1-2,i}$, $\vec{\Pi}_{3-4,i}$ contributions as defined in Refs. [1-4]. Using a scaling relevant to the tokamak edge, $\varepsilon \sim B_\theta/B_\phi \sim (qRv_{Tj}/c_j)^{-1} \sim L_\psi/r \sim r/(qR)$, and by taking the toroidal projection of (2) and averaging over a flux surface, one finally gets the toroidal momentum equation for plasma with circular cross sections

$$\begin{aligned} m_i N_i (1+2q^2) \frac{\partial}{\partial t} U_{\theta,i} = & q^2 m_i \langle \tilde{Z} \cos \theta \rangle U_{\theta,i} - \frac{3\eta_{0,i}}{2R^2} \left(U_{\theta,i} + 1.833 (e_i B_\phi)^{-1} \frac{\partial \Gamma}{\partial r} \right) + 0.54 \frac{\eta_{2,i}}{1+Q^2/S^2} q^2 \\ & \times \frac{e_i B_\phi}{T_i} \frac{\partial \ln T_i}{\partial r} \left[\frac{T_i}{e_i B_\theta} \frac{\partial U_\phi}{\partial r} + \frac{1}{2} U_{\phi,i}^2 - U_{\phi,i} \frac{B_\phi}{B_\theta} \left(U_{\theta,i} - \frac{T_i}{e_i B_\phi} \frac{\partial \ln N_i^2 T_i}{\partial r} \right) + 1.90 \frac{B_\phi^2}{B_\theta^2} \left(U_{\theta,i} - 0.8 \frac{T_i}{e_i B_\phi} \frac{\partial \ln N_i^{1.6} T_i}{\partial r} \right)^2 \right] - J_r B_\theta \end{aligned} \quad (3)$$

where \tilde{Z} is the poloidal angle dependent part of $Z = S_i^N - J^{-1} \partial_\psi (h_\phi h_\chi \Gamma_{\psi,i})$ which may lead to the Stringer spin-up for a suitable θ dependence of the source and $Q = [4B_\phi U_{\theta,i} - 2.5(T_i/e_i) \partial \ln N_i^2 T_i / \partial r] B^{-1}$ and $S = (2r\chi_{\parallel,i} N_i^{-1}) / (q^2 R^2)$, where the parallel heat diffusion coefficient is $\chi_{\parallel,i} = 3.9P_i / m_i v_i$. Likewise, one can obtain the neoclassical ambipolarity equation as [1, 2]

$$m_i N_i \frac{\partial U_{\phi,i}}{\partial t} = \frac{\partial}{\partial r} \left[\eta_{2,i} \left(\frac{\partial U_{\phi,i}}{\partial r} - \frac{0.107q^2}{1+Q^2/S^2} \frac{\partial \ln T_i}{\partial r} \frac{B_\phi}{B_\theta} U_{\theta,i} \right) \right] + J_r B_\theta \quad (4)$$

Above system (3-4) represents a two-time-scales problem, namely, it depends on a fast time variable $\tau = t/\varepsilon^2$, as well as a macroscopic time t . A solution procedure for this problem was suggested in Ref. [3] specializing r to a boundary layer inside the magnetic separatrix by

$\xi=(r-r_s)/L_\psi$. A smooth temperature profile model and a density profile connected to it, depending on parameters μ , T_c/T_s , Δ , forming a realistic steepness before the separatrix is taken with this system. After normalization with the values of the variables at the position of the magnetic separatrix, we obtain

$$\hat{N} \frac{\partial \hat{U}_\theta}{\partial \hat{t}} = \frac{\partial}{\partial \xi} \left[\hat{\eta}_2 \frac{\partial \hat{U}_\theta}{\partial \xi} - G \hat{U}_\theta \right] + \hat{N} (\hat{m} - \hat{v}_{cx} \hat{U}_\theta) + J_r B_\theta [t_{ref} / (m_i N_s \mu v_{th})] \quad (5)$$

$$\text{here } \hat{N} = \hat{T}^\gamma, \quad G = \hat{\eta}_2 \frac{0.107q^2}{1 + \frac{Q^2}{S^2}} \frac{\partial \ln \hat{T}}{\partial \xi} \quad \text{and} \quad \hat{\eta}_2 = 1.2 \hat{N}^2 \hat{T}^{-1/2}.$$

A basic assumption made above was that

$$\frac{t_{ref}}{m_i N_s} \frac{\eta_{2,ref}}{L_\psi^2} \approx 1. \quad (6)$$

Dropping the symbol, “^”, for normalization and using the logarithmic derivative we can write

$$\frac{\partial}{\partial \xi} (G U_\theta) = G U_\theta \left\{ \frac{U_\theta'}{U_\theta} + \frac{\eta_2'}{\eta_2} + \left(\frac{T''}{T'} - \frac{T'}{T} \right) - 2 \frac{(Q/S)^2}{1 + (Q/S)^2} (Q'/Q - S'/S) \right\}$$

Since other normalized terms were $Q = 4 \times [U_\theta - 0.625(2\gamma + 1)T']$ and $S = 4 \times 1.95 T^{2.5-\gamma}$,

$$\begin{aligned} \frac{\partial}{\partial \xi} (G U_\theta) = G U_\theta \left\{ \frac{\eta_2'}{\eta_2} + \left(\frac{T''}{T'} - \frac{T'}{T} \right) + \frac{2(Q/S)^2}{1 + (Q/S)^2} \left[(2.5 - \gamma) \frac{T'}{T} + 0.625(2\gamma + 1) \frac{T''}{Q} \right] + \right. \\ \left. + \left(\frac{1}{U_\theta} - 2 \frac{Q/S^2}{1 + (Q/S)^2} \right) \frac{\partial U_\theta}{\partial \xi} \right\} \end{aligned}$$

Similarly, the normalized parallel momentum equation becomes

$$\begin{aligned} \hat{N}(1 + 2q^2) \frac{\partial \hat{U}_\theta}{\partial \hat{t}} = \left(\frac{t_{ref}}{m N_{ref}} \frac{-3\eta_{0,ref}}{2R^2} \right) \hat{\eta}_0 \left\{ (\hat{U}_\theta + 1.833 \frac{\partial \hat{T}}{\partial \xi} + \Delta) + \right. \\ \left. \left(\frac{0.54\eta_2}{1.5\eta_0} \frac{R^2}{\mu L_\psi^2} \frac{B_\phi}{B_\theta} \right) \frac{q^2}{1 + \frac{Q^2}{S^2}} \frac{1}{\hat{T}} \frac{\partial \ln T}{\partial \xi} \left[- \hat{T} \frac{\partial \hat{U}_\theta}{\partial \xi} - \frac{1}{2} \hat{U}_\theta^2 + \hat{U}_\theta (\hat{U}_\theta - \hat{T} \frac{\partial \ln \hat{N}^2 \hat{T}}{\partial \xi}) \right. \right. \\ \left. \left. - 1.9 (\hat{U}_\theta - 0.8 \hat{T} \frac{\partial \ln \hat{N}^{1.6} \hat{T}}{\partial \xi})^2 \right] \right\} - J_r B_\phi / (\mu^2 v_{th}) \quad (7) \end{aligned}$$

Considering

$$\frac{\eta_2}{\eta_0} = \frac{6}{5 \times 0.94} \left(\frac{v_i}{\Omega_i} \right)^2 = \frac{6}{5 \times 0.94} \varepsilon^6 \hat{T}^{-3} \hat{N}^2 \quad (8)$$

and our assumption for t_{ref} , in (6), the factor to the right of the curly brackets Eq. (6) is found as $\frac{-3 \times 5 \times 0.96}{2 \times 6} \varepsilon^{-2} \hat{\eta}_0$. Since, $\hat{\eta}_0 = 0.96 \hat{T}^{5/2}$, the factor before the square brackets in Eq. (7) is found from (8), as

$$\frac{0.45}{1 + Q^2/S^2} T^{-4+2\gamma} \frac{\partial T}{\partial \xi}. \quad (9)$$

3. Treatment as a Nonlinear Dynamical System

If the spatial dependence is discretized, the partial differential equations (5) and (7) can be cast into the form of a dissipative dynamical system for the unknown average velocity components U_ϕ and U_θ , taken at the grid nodes, as $U = [U_{\phi,1}, U_{\theta,1}, \dots, U_{\phi,N}, U_{\theta,N}]$, and $U \in \mathbb{R}^{2N}$, where N is the number of grid points. The discretization must take into account of the radial boundary layer of U and the profile of the temperature pedestal just inside of the magnetic separatrix.

A standard model system for such studies is the Brusselator reaction kinetic scheme [6, 7, 9]. One of the crucial points in such a scheme is the treatment of the boundary conditions. If the zone of the radial discretization can be extended into the limits of zero or small gradients, one can assume the so called, “zero-flux” boundary conditions, i.e.:

$$\begin{aligned} U_{\phi,0} &= U_{\phi,1}, & U_{\phi,N+1} &= U_{\phi,N}, \\ U_{\theta,0} &= U_{\theta,1}, & U_{\theta,N+1} &= U_{\theta,N}. \end{aligned} \quad (10)$$

In the following, we shall adopt this point of view. The temperature profile can be approximated as a sum of n special monotonic functions of the radial coordinate, ξ :

$$T(\xi) = T_s \sum_{i=1}^n A_i [1 - y_i(\xi)], \quad \text{where } y_i = \tanh(a_i + \xi/\mu_i) \quad (11)$$

where A_i , a_i , and μ_i are constants and T_s is the temperature at the separatrix. Functions y_i have the property $y_i' = \mu_i^{-1} (1 - y_i^2)$ and $y_i'' = -2\mu_i^{-2} y_i (1 - y_i^2)$. Normalizing at the separatrix and somewhere beyond the pedestal, or the core side (say, at C), we obtain two relations among the coefficients as $1 = \sum_{i=1}^n A_i [1 - \tanh(a_i)]$ and $T_c/T_s = 2 \sum_{i=1}^n A_i$ where T_c is the temperature at core. For example, ALCATOR C-MOD temperature data of Ref. [4] can be approximated as in Fig.(1) choosing $n=3$, and the constants in $y_i(\xi)$ as $A_1=0.7$, $A_2=2.19$; $a_1=0.3$, $a_2=1.5$; $\mu_1=1.0$, $\mu_2=8.85$, $\mu_3=0.5$. The solid line in Fig.1., is the approximation given in Eq.(11) for $n=3$. A temperature pedestal T_p can be clearly seen to exist at about $\xi \approx -2$. Notice that the present model yields an adequate approximation also in the SOL. However, for the computational economy, we can simulate the temperature profile also by a single control parameter of steepness, μ , and express T , simply as $T(\xi) = 0.5 T_c [1 - \tanh(a + \xi/\mu)]$, where $a = \tanh^{-1}(1 - 2T_s/T_c)$, $T' = -(2/\mu) T [1 - (T_s/T_c) T]$, $T'' = (2/\mu)^2 T [1 - (T_s/T_c) T] [1 - 2(T_s/T_c) T]$.

4. Simulations

We present here our computational results for the variation of rotation velocity components over the interval $-7 < \xi < 1$, assuming that the velocity gradients at both ends of the interval are sufficiently small. The convergence of the numerical results can be checked using an increasing number of nodes (for example, taking $N=5, 10, 15, \dots$) in the calculation of fixed

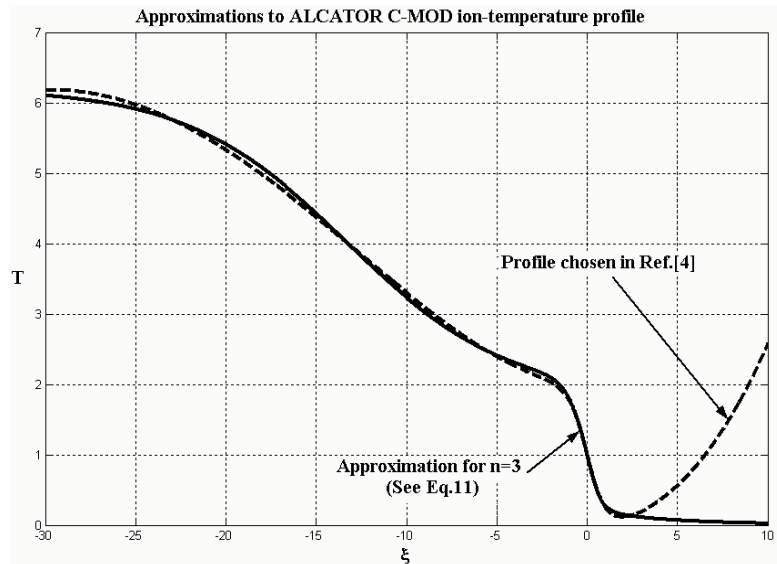


FIG.1. A model temperature profile controlled by 3 parameters simulating Alcator experiments.

points of the dynamical system, which represent its steady-state solutions. At each fixed point, we can then examine numerically the eigenvalues of the $2N \times 2N$ dimensional Jacobian and so classify the fixed points. A further observation gives information about the branching behaviour of the fixed points and their bifurcation in the $2N+1$ dimensional extended-state space. Results of such a study can be summarized as shown in Fig.2. on the $([U], \mu)$ plane. To obtain a further detailed look on bifurcations defining proper Poincaré sections, is rendered difficult, as any periodic solutions for the unknowns are not known. However, it is illuminative to compare the individual (velocity component, vs μ) figures computed at different locations represented now by indices. We present on Figs. 3-6 some of these plots calculated at near and far distances from the separatrix. It is important to note that the steady-state solutions for poloidal velocity profiles are very sensitive to distance (or index)

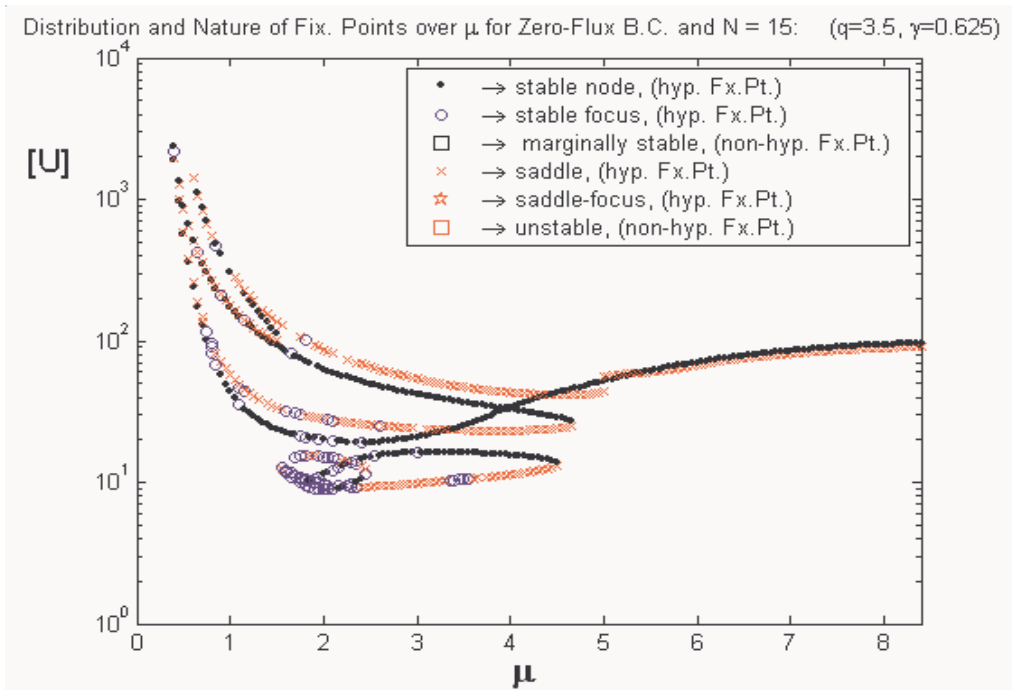


FIG.2. In a representative μ -interval, the distribution and the nature of the fixed points of the dynamical system as calculated over $(-7 < \xi < 1)$ with $N=15$.

from the separatrix indicated by strong topological changes. Whereas, the toroidal velocity component lack such a variability.

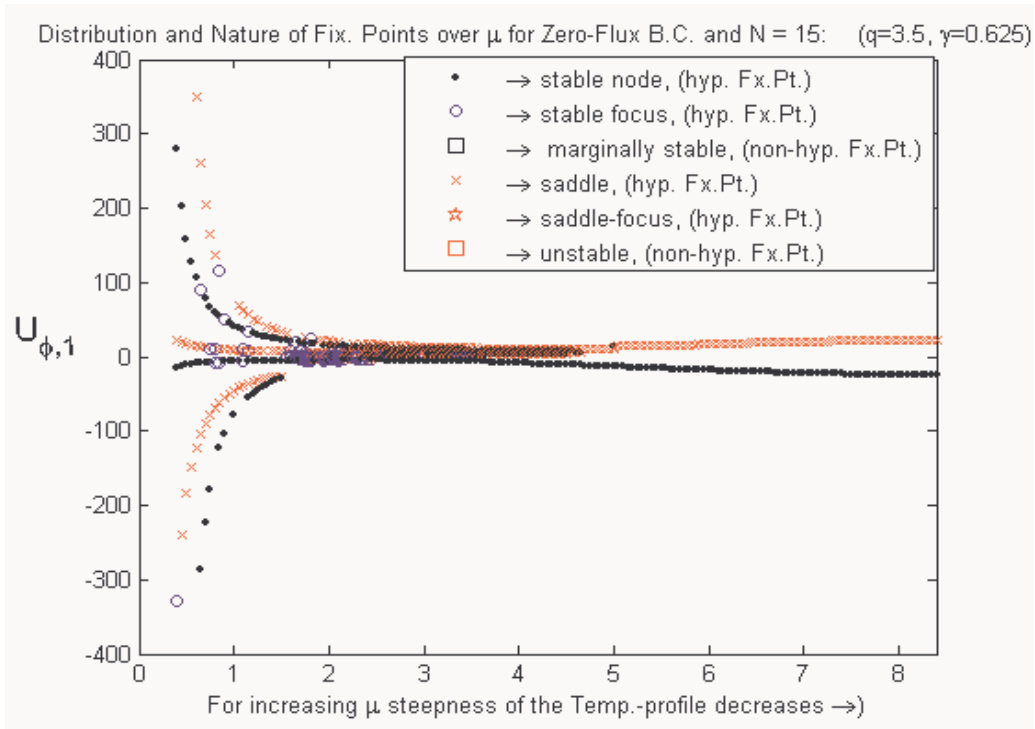


FIG.3. Topology of the fixed point distributions on $(U_{\phi,i}, \mu)$ planes are very similar. Hence, only one of them is given.

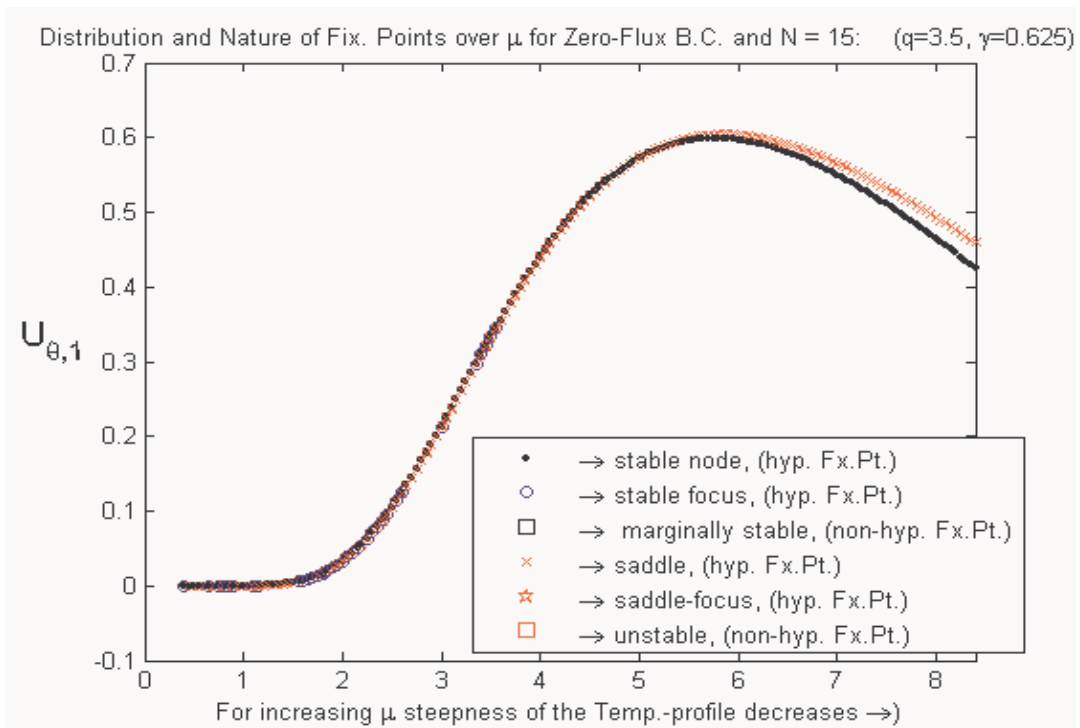


FIG.4. Increasing distance from the separatrix through the core simplifies the topology of the fixed point distribution in the (U_{θ}, μ) plane.

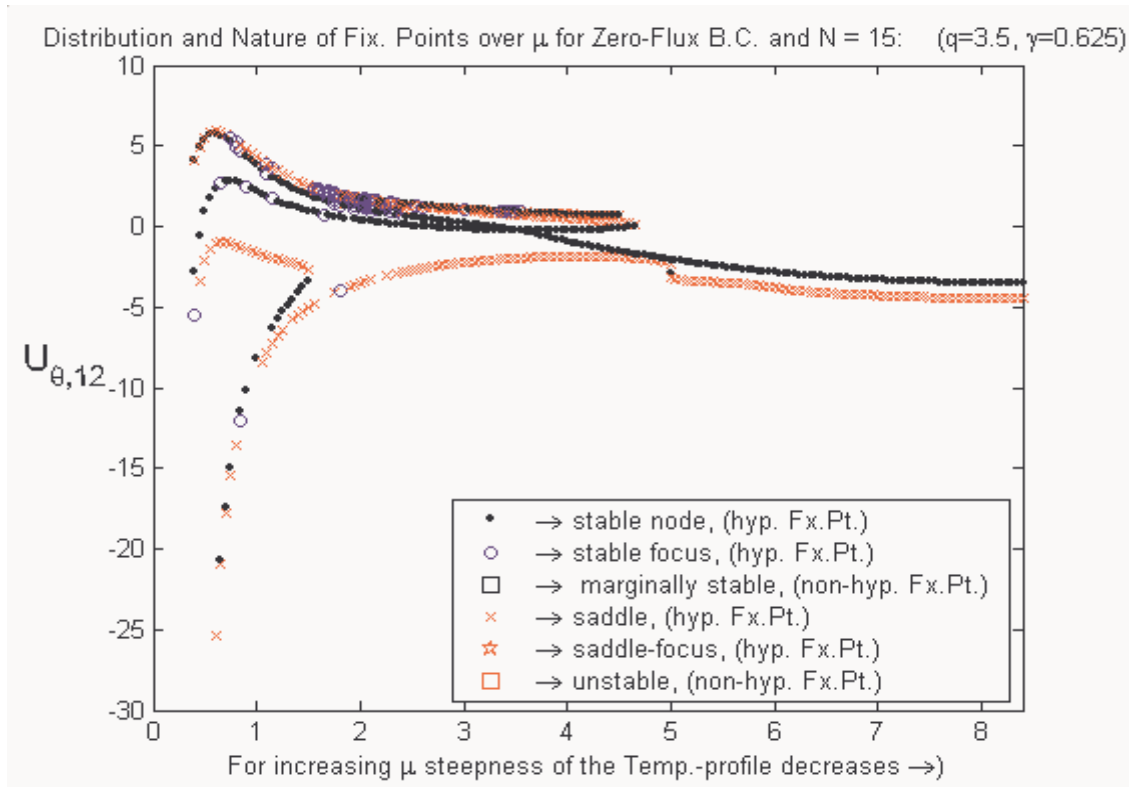


FIG.5. Comparing with Fig.4., one observes a strong dependence of fixed point distribution on index or position in (U_θ, μ) plane.

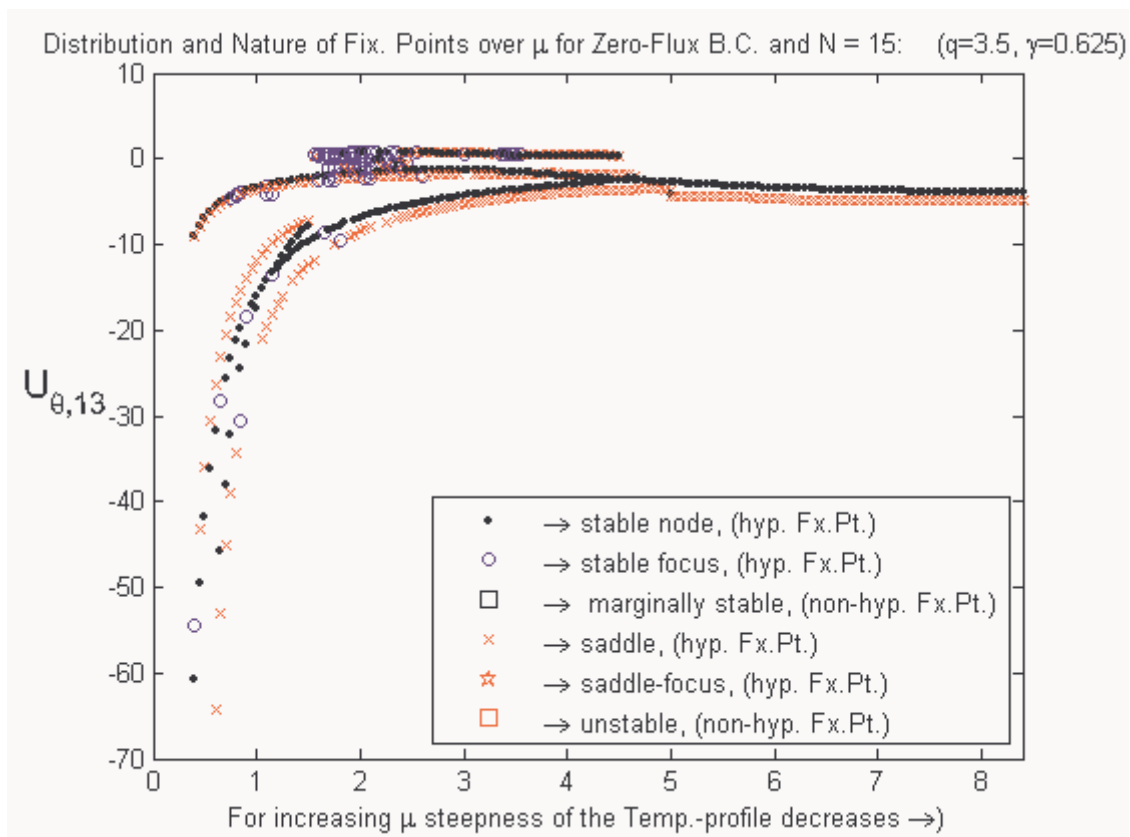


FIG.6. Comparison with Fig.5., shows, that even a small variation of index or position near the separatrix causes great change in the fixed point distribution in (U_θ, μ) plane.

5. Discussion of the Results

Computations presented above were performed using MATLAB 6.5 and 7.0 Versions and their program library. As the problem described above constitutes a multi-dimensional dynamical system, it is difficult to construct the Poincaré sections as one does not have a complete a priori picture of the state-space. A search for the fixed points of the system reveals the possible steady-states of the system (Fig.1.), although some of them, depending strongly on the steepness of the temperature gradient inside the separatrix, may be unstable, as a subsequent analysis of the eigenvalues indicate. A numerical code developed for this purpose can analyse the eigenvalues of the Jacobian at each fixed point and classify them. As the poloidal velocity components display in the neighborhood of the separatrix a large topological sensitivity to the steepness parameter, μ , the important dynamical features of the system can be understood from their study. For this purpose the grid-node number N , must be sufficiently high, although it would also raise the computational efforts sharply. From Figs. 4,5 we infer that the decrease of μ , further down from 0.5, causes a loss of characterization of the fixed points, as various branches merge. On the same figures one notices also several bifurcations, including also a global one for the components near the separatrix position. As stated above, the toroidal velocity components at all positions display a similar dependence on the temperature steepness, and loose definition as the steepness is increased for $\mu < 0.5$.

References

- [1] REGISTER, A., "Revisited Neoclassical Transport-Theory for Steep, Collisional Plasma Edge Profiles", *Physics of Plasmas* **1** (1994) 619.
- [2] CLAASSEN, H. A., et al., "Neoclassical Theory of Rotation and Electric Field in High Collisionality Plasmas with Steep Gradients", *Physics of Plasmas* **7** (2000) 3699.
- [3] DAYBELGE, U., YARIM, C., and NICOLAI, A., "Rotation Dynamics and Stability of Collisional Edge Layers in Tokamak Plasma", *Nuclear Fusion* **44** (2004) 966.
- [4] NICOLAI, A., DAYBELGE, U., YARIM, C., "Modelling of Plasma Rotation Accounting for a Poloidal Divertor and Helical Perturbation Coils", *Nuclear Fusion*, **46** (2006) S145.
- [5] MIKHAILOWSKII, A.B., TSYPIN, V.S., *Beitr. Plasmaphys.* **24** (1984) 335.
- [6] MAREK, M., SCHREIBER, I., "Chaotic Behaviour of Deterministic Dissipative Systems", Cambridge Univ. Press (1995) Prague.
- [7] SEYDEL, R., "Practical Bifurcation and Stability Analysis, From Equilibrium to Chaos", Sec. Edition., Springer-Verlag, (1994), New York, Berlin, Heidelberg.
- [8] NAYFEH, A. H., and BALACHANDRAN, B., "Applied Nonlinear Dynamics", Wiley-Interscience, John Wiley & Sons, Inc. (1995) New York.
- [9] NICOLIS, G. and PRIGOGINE, I., "Self Organization in Non-Equilibrium Systems. From Dissipative Structures to Order Through Fluctuations", Wiley (1977) New York..